NCURO Data-Retrieval Algorithm in FORMOSAT-3 GPS Radio-Occultation Mission

Tsen-Chieh Chiu, *Member, IEEE*, Yuei-An Liou, *Senior Member, IEEE*, Wen-Hao Yeh, and Cheng-Yung Huang

Abstract—Radio-occultation (RO) technique, which has been used in planetary science, is a method to obtain the profiles of atmosphere and the global atmospheric data. In 2006, Taiwan launched six low-Earth-orbit satellites as a RO constellation mission, known as FORMOSAT-3. In order to thoroughly understand the process of the RO data retrieval and obtain as much as possible the information for the weather prediction, a National Central University Radio Occultation (NCURO) retrieval algorithm has been developed. The focus of the algorithm development is on the correction of the excess phase of the signal received with open-loop (OL) technique and the criteria for assessment of the data quality. When the OL is activated, the excess phase of the global-positioning-system (GPS) signal is modulated with navigation messages of satellites. In our algorithms, two methods are incorporated to recover the excess phase. Moreover, as the altitude of the received signal decreases, the quality of the GPS signal generally deteriorates, and eventually, the signal is too noisy to be processed. In order to assess the quality of the signal, instead of the signal-to-noise ratio, the degree of unclearness is defined and used in the algorithm. In this paper, the algorithm including the phase-correction methods and the criteria for the quality assessment will be described. The data retrieval using the algorithm will be compared with those obtained from the COSMIC Data Analysis and Archive Center at the University Corporation for Atmosphere Research and Pingtung radiosonde measurement. Some intermediate results of the NCURO algorithm will also be demonstrated.

Index Terms—Global positioning system (GPS), open loop (OL), radio occultation (RO).

I. INTRODUCTION

RADIO-OCCULTATION (RO) technique has been applied to investigate the atmosphere of planets in the solar system for decades [1]–[4]. It is based on the fact that the radio waves are bent and delayed due to the gradient of the atmospheric refractivity along the ray path. By analyzing the excess phase of the radio waves, the profiles of atmospheric parameters can be retrieved. With the advent of global positioning system (GPS), it becomes possible to retrieve the refractivity and temperature profiles of the Earth's atmosphere using the occultation technique. The first RO satellite, MicroLab-1, was launched in 1995. It receives the GPS signal and creates about 500 RO data per day. Because it is not limited by weather and topography, the RO technique can provide much information to monitor the variation of the global temperature [5]. Since the operation of MicroLab-1, many satellites of RO missions have been launched, such as CHAMP [6], [7] and GRACE [8].

In 2006, Taiwan launched six low-Earth-orbit (LEO) satellites for a RO mission. The name of the mission is Constellation Observing System for Meteorology, Ionosphere and Climate (FORMOSAT-3/COSMIC or FORMOSAT-3). FORMOSAT-3 is a cooperative mission between Taiwan and the U.S. The executive organizations in Taiwan and the U.S. are the National Space Organization and University Corporation for Atmosphere Research (UCAR), respectively. The amount of the RO data supplied by FORMOSAT-3 is expected to be 2500–3000 sets per day. The RO data provided by FORMOSAT-3 can be applied to monitor and study the dynamic of ionosphere [9]–[11], the space weather [12], [13], the structure of atmosphere [14]–[18], the gravity of the Earth [19], and the gravity wave [20]. The RO data can also be provided to improve the accuracy for weather prediction [21]. The RO data of FORMOSAT-3 are freely provided by Taiwan Analysis Center for COSMIC (TACC) and COSMIC Data Analysis and Archive Center (CDAAC) at UCAR.

There have been several algorithms to retrieve atmospheric parameters from the RO data, such as the algorithm developed by UCAR [22]. These algorithms are mainly based on methods such as the geometrical method [23], [24], the back-propagation method [25], [26], the holographic method [27], [28], the amplitude-retrieval method [29], the full-spectrum-inversion method [30], and the canonical transformation [31]. In addition, many operations such as data-filtering, smoothing, and empirically weighting methods are involved in the algorithms. It is suspected that some atmospheric information could be lost through these operations. In order to thoroughly understand the process of the data retrieval and obtain as much as possible the information for the weather prediction, a retrieval algorithm, the National Central University Radio Occultation (NCURO) algorithm, is developed [32], [33]. Based on the geometrical method, the NCURO algorithm uses the excess phase of the GPS signal to obtain the profiles of atmospheric pressure and temperature.

One of the many focuses of FORMOSAT-3/COSMIC is the investigation of the atmospheric phenomena at low altitude (generally below 10 km). These phenomena are
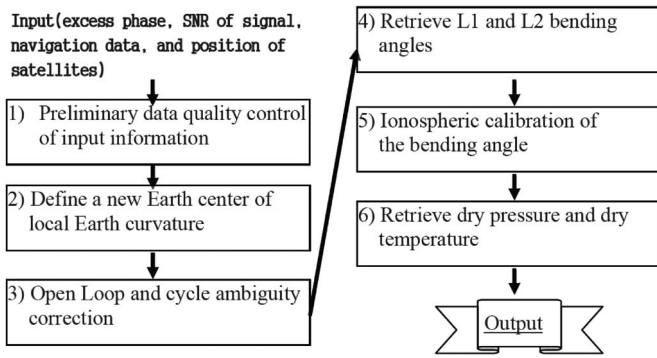
T.-C. Chiu and W.-H. Yeh are with the Department of Electrical Engineering, National Central University, Taoyuan 320, Taiwan.

Y.-A. Liou is with the Department of Electrical Engineering and the Center for Space and Remote Sensing Research, National Central University, Taoyuan 320, Taiwan.

C.-Y. Huang is with the Institute for Scientific Research, Boston College, Chestnut Hill, MA 02467 USA.

Fig. 1. Flowchart of the NCURO data-retrieval algorithm.

Fig. 2. Modulation of the GPS signal. The carrier and the code of the GPS signal are combined using PSK.

essential for climatic modeling and weather prediction. When the GPS signal is transmitted through the low-altitude atmosphere, the multipath and strong fluctuation of the signal caused by moist troposphere could deteriorate the quality of data. In FORMOSAT-3 data, the open-loop (OL) technique [2], [15], [34] is used to replace the traditional phase-locked loop (PLL) technique to track the GPS signal at low altitude. Basically, the OL technique uses a frequency filter with the predefined bandwidth to ensure the signal receiving [34]. However, with OL, the phases of the GPS signals are affected by the navigation message. The phases must be corrected before further processing. Moreover, the quality of the GPS data deteriorates as the altitude decreases, which eventually weakens the GPS signal too much for the algorithm to proceed. The data quality is the main factor which determines the lowest altitude of the retrieved parameter profiles. Therefore, criteria for the quality of the GPS signal must be set up. In what follows, the NCURO algorithm is first summarized in Section II. In Section III, two correcting methods developed to remove the effect of the navigation message on the excess phase of the signal are described. In Section IV, the degree of unclearness is defined and applied to determine the quality of the signal. The comparisons of the retrieved results are displayed in Section V, followed by the conclusion.

II. RETRIEVAL ALGORITHM OF GPS RO DATA

Fig. 1 shows the flowchart of the NCURO data-retrieval algorithm. Following the algorithm, the dry-pressure and temperature profiles of atmosphere can be retrieved from the GPS signals. The main input parameters of the algorithm are the excess phase, signal-to-noise ratio (SNR) of the GPS signal, navigation-data modulation bits, and the position data of GPS and LEO satellites. All the input data can be obtained in atmPhs and gpsBit files from COSMIC postprocessed data in TACC. The gpsBit files contain GPS navigation-data modulation bits [35]. The atmPhs files contain the excess phase, SNR of the GPS signal, and the position data of GPS and LEO satellites. Both gpsBit and atmPhs files are named using the rule explained in the example of atmPhs_C001.2006.239. 02.30.G30_0001.0001_nc, where

atmPhs	could also be gpsBit;
C001	number of Formosat-3/Cosmic satellites;
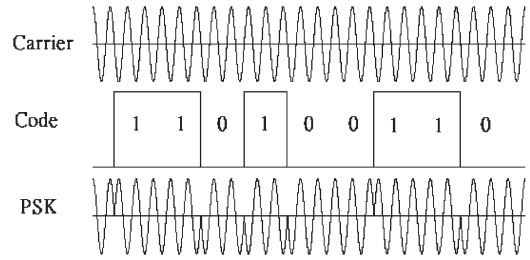
2006.239.02.30	year, day of year, hour, and minute when the file is recorded;
G30	number of the GPS satellites (GNSS id);
0001.0001	(first) ID which tells the command options used in generating this file and (second) ID which tells the version of all codes used in generating this file;
nc	data format of the file.

More details regarding the data format can be found in [34]. In what follows, the details of each step in the algorithm are described.

The first step of the algorithm, the preliminary data quality control, is to assess the data integrity of the input parameters. If the integrity does not meet the expectation, the algorithm will stop. In the preliminary data quality control, two factors are mainly considered: the number of the data points in data sequence and the mean SNR of the GPS signal in a preselected altitude range. If, in the preselected range, the number of RO points is insufficient or the mean SNR of the GPS signal is low, the algorithm will not continue. In the algorithm, the typically preselected altitude range is chosen from 40 to 60 km. Following the determination of the data integrity, the process of the data retrieval begins. In the NCURO algorithm, the atmosphere of the Earth is assumed to be spherically multilayered. However, in practice, due to the oblateness of the Earth, this assumption is inaccurate. With this assumption, the retrieved temperature below the altitude of 40 km may possess a bias. Generally, the bias is about 3 K at 10 km in altitude and 6 K on the ground [37]. To remove the bias, Syndergaard's method [37] is applied to obtain a new local radius of the Earth. The effect of the oblateness of the Earth is thus eliminated.

GPS signals are transmitted at two frequencies: 1575.42 MHz (L1) and 1227.60 MHz (L2). The signals are modulated with the navigation message using phase-shift-keying (PSK) technique to provide satellite clock readings to the receiver and to transmit information such as the orbital parameters [38], [39]. When the signal propagates through the moist troposphere, multipath and strong fluctuation in phase and amplitude of the signal could deteriorate the data quality. Fig. 2 shows a typical modulated GPS signal. The phase shifts $180°$ when the code changed. Traditionally, PLL, which uses negative feedback to track signal frequency, is applied to correct the phase shift. However, if the signal becomes weak, PLL may not be able to track the signal correctly. The information embedded in the phase could be damaged.

Recently, the OL technique is used to circumvent the situation when PLL fails. OL uses a precalculated model to replace the feedback signal and to ensure the receiving of the GPS signal. Nevertheless, to calculate the bending angles from the excess phase of the GPS signal received with OL, ambiguity in phase will happen due to the modulation of the navigation message. The correction methods with regard to the phase-ambiguity removal will be described in Section III.

With the corrected excess phase, the bending angle of the GPS signal can be calculated. The bending angle is equal to the angle between two vectors. One of the vectors is from the center of the Earth to the point where the GPS signal impinges on the atmosphere. The other vector is from the center of the Earth to the point where the GPS signal leaves the atmosphere. Following the Snell's law, it is found that the lengths of both vectors are equal to the value of impact parameter. Then, the bending angles of L1 and L2 GPS signals can be calculated using geometric-optic technique [40]. When obtaining the bending-angle profile in the neutral atmosphere, the ionosphere is considered as a source of noise to the signal. Since the refractive index of the ionosphere is related to the concentration of electrons and the frequency of electromagnetic wave, the L1 and L2 signals can be combined to significantly reduce the effect of the ionosphere. In the NCURO algorithm, the atmospheric bending angle is calculated using [41]

$$\alpha(r) = \frac{f_1^2 \alpha_1(r) - f_2^2 \alpha_2(r)}{f_1^2 - f_2^2} \qquad (1)$$

where f_1 is the frequency of L1, f_2 is the frequency of L2, α_1 is the bending angle of L1, α_2 is the bending angle of L2, α is bending angle after ionospheric correction, and r is impact parameter. In (1), α_1 and α_2 are matched to the same impact parameter r. Due to the multipath, moisture, and other influence, the quality of the L2 signal in the troposphere is often poor. Therefore, the data of the L2 bending angle may not be available at low altitude.

The next step is to obtain the refractivity (N) of the atmosphere. Abel transform [42], which is often used to analyze the axially symmetric or spherically symmetric functions, is applied to transfer the bending angle to the refractivity of the atmosphere. The equation of Abel transform used in RO technique is written by

$$n(r_p) = \exp\left[\frac{1}{\pi}\int_{r_p}^{\infty} \frac{\alpha(a)}{\sqrt{a^2 - a_p^2}}\, da\right] \qquad (2)$$

where $n(r_p)$ is the refractive index at r_p, r_p is the altitude of perigee, a is impact parameter, a_p is the impact parameter at perigee $(a_p = n(r_p)r_p)$, and $\alpha(a)$ is the bending angle at a. Moreover, the relation between refractivity and refractive index is $N = (n-1) \times 10^6$. Then, the pressure and temperature profiles of the atmosphere can be obtained in the following procedure.

1) As the frequency of the signal is under 20 GHz [23], the refractivity of the atmosphere can be expressed in terms of the gas temperature T (in Kelvin), dry pressure P_d (in millibars), and wet pressure P_w (in millibars) [43]

$$N = k_1 \frac{P_d}{T} + k_2 \frac{P_w}{T} + k_3 \frac{P_w}{T^2} \qquad (3)$$

where $k_1 = 77.604$ K/mbar, $k_2 = 64.79$ K/mbar, and $k_3 = 3.776 \times 10^5$ K^2/mbar.

2) There are two unknowns, P_d and P_w, in (3). Compared to P_d, P_w is significantly smaller at high altitude (> 10 km). To simplify the computation, P_w is neglected in the NCURO algorithm. Substituting the static hydrodynamic equation $dP = -g\rho dz$ into (3), the dry pressure is given by

$$P_d(z_i) = \frac{M}{77.6R} \int_{z_i}^{\text{Top}} -g(z)N(z)dz + P(\text{Top}) \qquad (4)$$

where g is the gravitational constant, R is the ideal gas constant, M is one mole weight of molecule, Top is the top of the atmosphere, and z_i is the altitude where P_d is calculated.

3) The dry temperature is given by

$$T(z_i) = 77.6 \frac{P_d(z_i)}{N(z_i)}. \qquad (5)$$

The outputs of the NCURO algorithm are dry pressure and dry temperature. Since P_w is neglected, the near-surface portions of atmospheric profiles may be inaccurate. To perform the correction, 1-D variation analysis using European Centre for Medium-Range Weather Forecasts (ECMWFs) low-resolution analysis data could be applied to obtain the atmospheric profiles of refractivity, temperature, and water vapor [44].

III. OL CORRECTION

As mentioned previously, PLL could fail when the signal is transmitted through the atmosphere at low altitude. In order to circumvent this problem, OL is used to replace PLL [34]. It can also resolve the random and systematic errors (bias) in the extracted phase and in the retrieved refractivity [45]. The phase of the signal tracked by OL is modulated with the navigation message. To obtain the correct excess phase of the signal, the navigation message must be removed. Two correction methods have been incorporated in the NCURO algorithm to correct the excess phase. In what follows, both methods will be described.

A. Method I: Correction With gpsBit File

The effect of OL on the bending angle is shown in Fig. 3. In Fig. 3, two bending-angle profiles without phase correction show large fluctuation at low altitude. In GPS signals, the phase shifts 180° when navigation-data modulation bit changes from one to zero or zero to one (as shown in Fig. 2). To obtain the correct excess phase, it is intuitive to just recover the phase shift according to the variation of the navigation-data
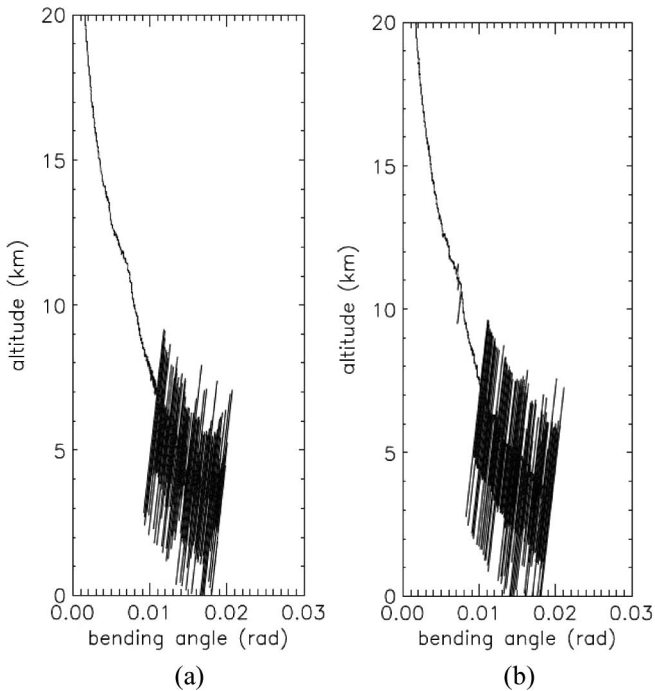
(a)   (b)

Fig. 3. Bending-angle profiles without phase correction. The profiles are retrieved from (a) atmPhs_C001.2006.239.02.30.G30_0001.0001_nc and (b) atmPhs_C004.2006.239.04.08.G21_0001.0001_nc, and the large fluctuation appears at low altitude once OL is activated.

modulation bits. However, the excess phase and navigation-data modulation bits are not recorded simultaneously in the gpsBit files. In addition, it is difficult to identify the starting bit of the navigation data in the phase of the GPS signal. To recover the excess phase, the signal and navigation-data modulation bits must be synchronized first. The procedure of the data synchronization is given as follows.

1) Transfer the phase of the GPS signal to the excess-phase rate (Doppler) [22]. One Doppler profile of the RO data is shown in Fig. 4 with the activation of OL. Multiple distinct lines appear in the figure.
2) Eliminate the atmospheric delay of the GPS signal in the Doppler profile. The increasing tendency in the Doppler profile disappears, and the profile becomes horizontal.
3) Select the portion of the Doppler profile where the GPS signal is received using OL. Assign the value of one to the data points of the middle line of the profile of multiple distinct lines. Assign zero to data points of the other lines. The result is shown in Fig. 5(a).
4) Repeat steps 1) and 3) on navigation-data modulation bits corresponding to the GPS signal shown in Fig. 4. The result is shown in Fig. 5(b).
5) Calculate the time correlation factor between the data in Fig. 5(a) and (b). The result is shown in Fig. 6.

The maximum value of the correlation factor is located at 0.6 s in Fig. 6. It is therefore found that the time lag is 0.6 s.

Fig. 7 shows two cases of the Doppler profiles (also used in Fig. 3) after phase correction. In Fig. 7(a) and (b), there are fluctuations due to low SNR of the signal. Even with OL,
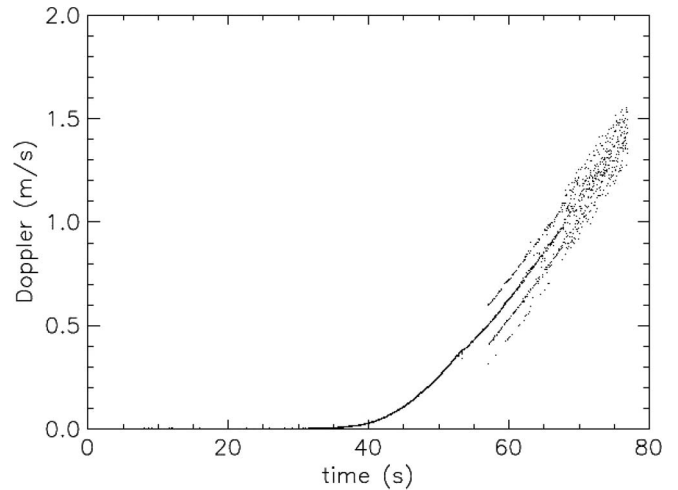

Fig. 4. Doppler of the RO excess-phase data. The multiple-line situation appears once OL is activated. The abscissa is the receiving time, and the origin indicates that the receiver begins to receive GPS signal.
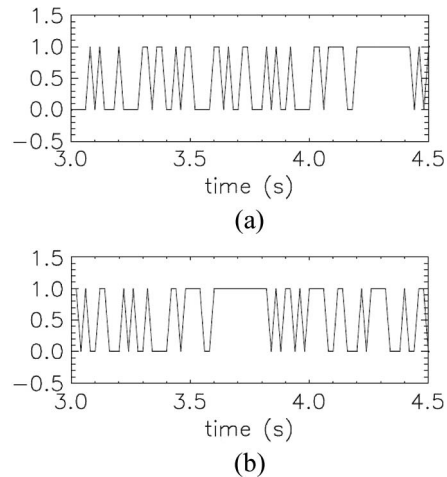

(a)

(b)

Fig. 5. (a) Transformed Doppler of the L1 signal from atmPhs_C001.2006.239.02.30.G30_0001.0001_nc. (b) Transformed navigation code from gpsBit_C001.2006.239.02.30.G30_0001.0001_nc. Comparing both figures, it is found that the signal in (a) is delayed by 0.6 s, which will be calculated in Fig. 6.
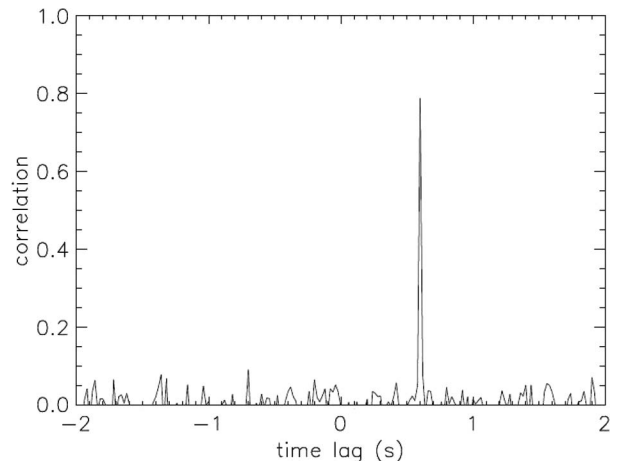

Fig. 6. Cross correlation between transformed Doppler and navigation data shown in Fig. 5. The time difference between the excess phase and navigation code is 0.6 s.
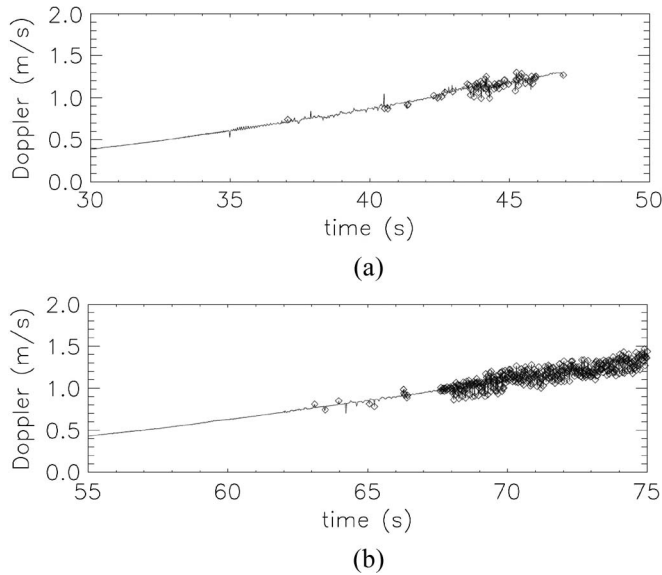
(a)

(b)

Fig. 7. Doppler profiles with phase correction using navigation code. The data are from (a) atmPhs_C001.2006.239.02.30.G30_0001.0001_nc and (b) atmPhs_C004.2006.239.04.08.G21_0001.0001_nc, and the squares indicate the data points of low SNR.
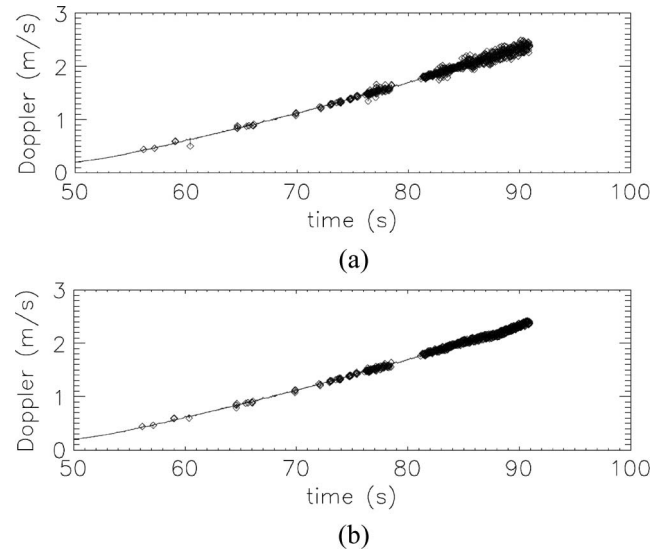

(a)

(b)

Fig. 9. Doppler profiles corrected by the phase-correction methods (a) with navigation code and (b) without navigation code. The squares indicate that the data of low SNR. The results of two correction methods are almost the same. The data are from atmPhs_C003.2006.195.02.49.G06_0001.0001_nc.

B. Method II: Correction Without gpsBit File

Sometimes, the navigation-data modulation bits recorded in the gpsBit file are incomplete. Somehow, some modulation bits are just not recorded in gpsBit files. Hence, the method I is not always applicable. Another method to correct phase without navigation-data modulation bits is proposed.

1) Perform steps 1) and 2) of the method I in the previous section.
2) In the GPS signal, phase shifts 180° as navigation-data modulation bit changes. In NCURO algorithm, it is found that the ordinate value of the data point resulted from step 1) is larger than 0.25 or less than −0.25 as the modulation bit changes. The correct excess phase can be obtained by adding 180° to the phase of the GPS signal if the corresponding data in step 1) is larger than 0.25 or subtracting 180° if less than −0.25.

The Doppler profiles after phase correction using methods I and II are shown in Fig. 9. Although method II is less complicated and easier to use, it is more susceptible to the phase noise. When SNR of the GPS signal is low, there is no way to tell if the phase shifts due to the change of the modulation bit. Generally, both corrected Doppler profiles are similar except for the data points with low SNR.
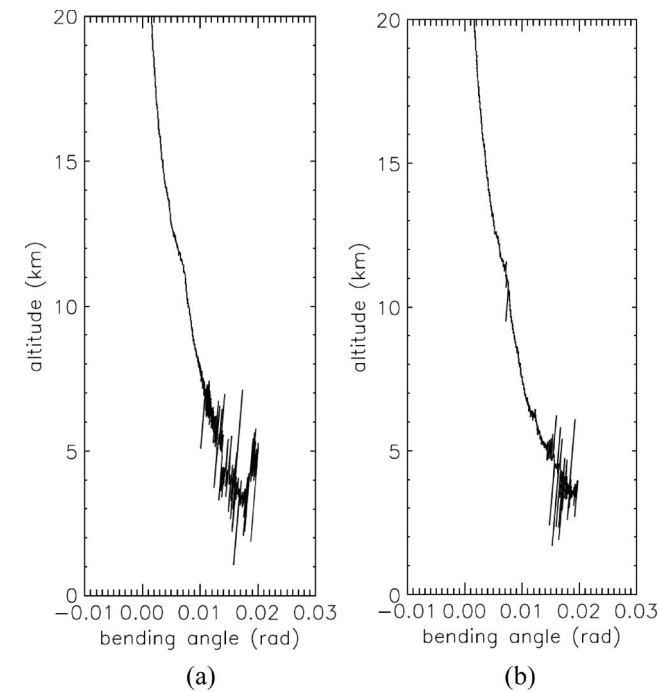

(a)

(b)

Fig. 8. Retrieved bending-angle profiles from atmPhs files used in Fig. 7.

IV. CRITERIA OF DATA QUALITY

The quality of the GPS signal generally deteriorates as the altitude decreases. It is important to find criteria with that the NCURO algorithm can determine which portion of the data should be discarded due to the poor quality. Intuitively, the SNR of the GPS signal can be used as a criterion for data quality. Figs. 10 and 11 show the excess phase and the corresponding SNR profiles of the L1 and L2 signals, respectively. As expected, the SNR decreases as the altitude decreases, and the data quality deteriorates. However, the SNR decreases with

the Doppler profiles at low altitude generally suffer from large noise, and the information of the excess phase is lost even with OL. These data of excess phase at low altitude cannot be recovered using the navigation-data modulation bits and will be discarded. Fig. 8 shows the profiles of the bending angle retrieved from the corrected excess-phase profiles. Compared with the profiles shown in Fig. 3, it is found that the multiple lines have converged into one, although there is still fluctuation due to low SNR of the GPS signal.
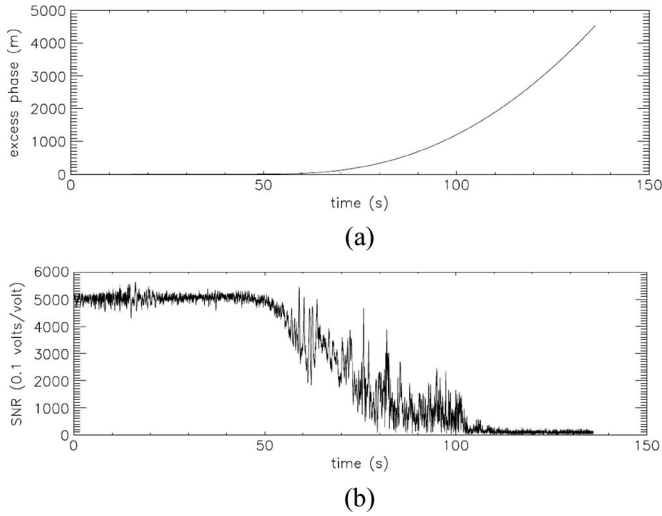
Fig. 10. (a) Excess phase of the L1 RO data and (b) its corresponding SNR profile. The data are from atmPhs_C001.2007.055.00.18.G14_0001.0001_nc.
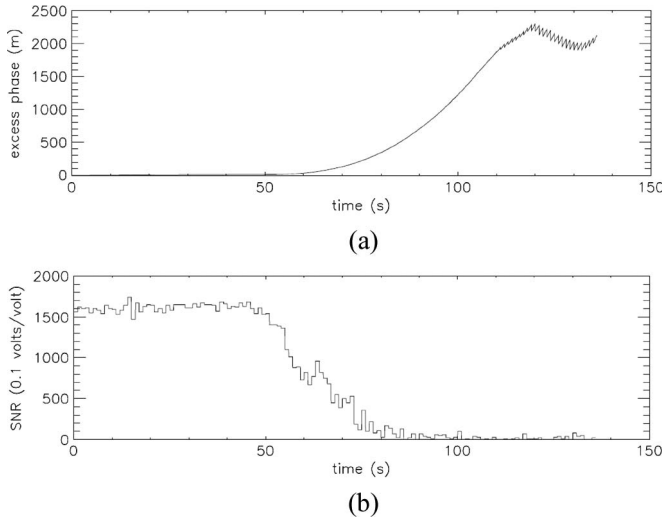

Fig. 11. (a) Excess phase of the L2 RO data and (b) its corresponding SNR profile. The data are from atmPhs_C001.2007.055.00.18.G14_0001.0001_nc.

fluctuation [example in Fig. 10(b)] which makes it difficult to locate the data of poor quality. Therefore, a new criterion will be set up in the algorithm.

The quality of the GPS signal cannot be easily examined in the data of the excess phase. However, it can be more easily examined in the Doppler profiles. Fig. 12(a) shows the Doppler profile of an L1 data. In the profile, the multiple-line situation due to the activation of OL gradually becomes indistinct and eventually distributes randomly. To quantify the quality of the phase data, the unclearness profile and the degree of unclearness are calculated and defined as follows.

1) Use the OL correction methods mentioned previously to obtain the Doppler profiles without the consideration of SNR. The result is shown in Fig. 12(b).
2) Perform the step 2) of the method I in Section III. The result is shown in Fig. 13(a).
3) Use the function $b = \cos(2\pi a)$ to transfer the data, where a and b are the value of the data points in Fig. 13(a) and (b), respectively.
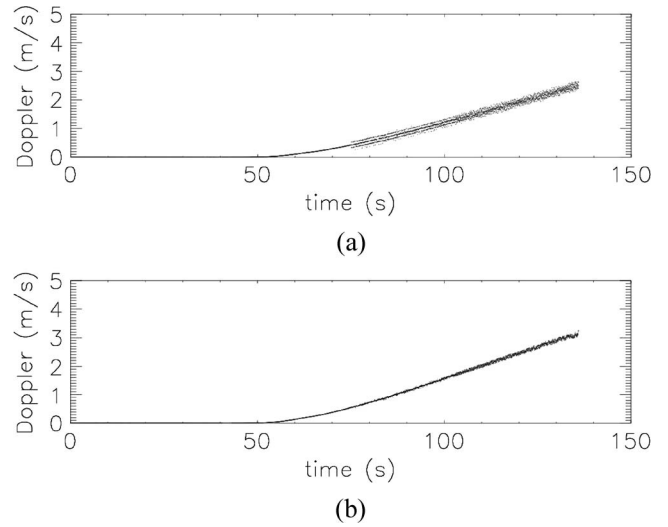

Fig. 12. (a) Uncorrected and (b) corrected Doppler of the RO data from atmPhs_C001.2007.055.00.18.G14_0001.0001_nc. In (b), the correction method is the method II in Section III (without navigation code).

4) Calculate the standard deviation of each data point in Fig. 13(b). The standard deviation of each data point is defined as the standard deviation of the nearest 50 points (which is decided by experience) from each side of the data point. The result is shown in Fig. 13(c).
5) Use the line-fitting technique to regress the data piece-wisely in Fig. 13(c). The result is shown in Fig. 13(d), which is the unclearness profile.

After considering several tens of data, the degree of unclearness is set to be 0.3 of ordinate. In the unclearness profile, if it is larger than the degree of unclearness, the corresponding data of the excess phase will be considered as data of poor quality. The main point of using the degree of unclearness is to reject the data of Doppler profile in Fig. 12(b) where the data points distribute randomly. When the quality of the data fails the criterion, it is considered that the receiver does not receive the GPS signal, and this portion of data must be rejected.

Unlike that of the L1 signal, the quality of the phase of the L2 signal can be examined in the Doppler profile easily. As shown in Fig. 14(a), the variation of the Doppler profile of the L2 signal at the end of the sequence is much larger than the other portion. It is easier to decide the degree of unclearness of the L2 signal than that of the L1 signal. It is only necessary to run the step 4) in the procedure aforementioned using the Doppler profile of the L2 signal. The result is shown in Fig. 14(b). The value of standard deviation rises abruptly when the data begin to distribute randomly. After considering several tens of data, the degree of unclearness is set at the point with 0.25 of ordinate.

V. COMPARISON WITH NCURO, TACC, AND RADIOSONDE DATA

The RO data provided by FORMOSAT-3 in January and February 2007 are processed and compared with the results obtained from atmPrf files in TACC and Pingtung radiosonde station in Taiwan. The data in atmPrf files are processed using the algorithm developed by CDAAC [27] at UCAR. The atmPrf
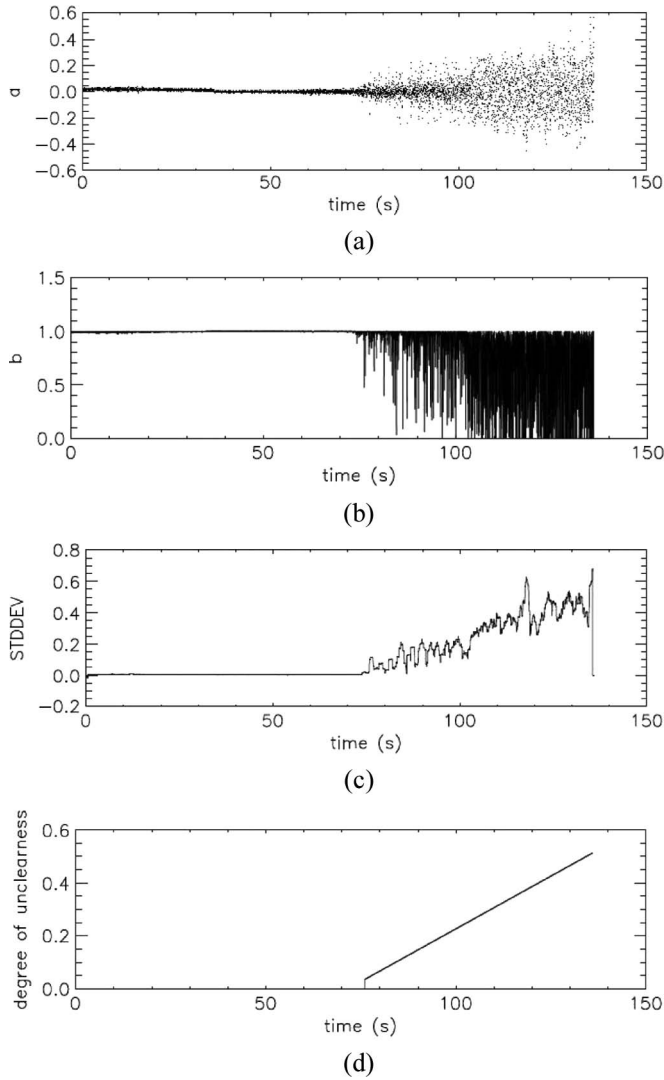
(a)

(b)

(c)

(d)

Fig. 13. Calculation of the degree of unclearness in Section IV. (a) and (b) are calculated results corresponding to the steps 2) and 3), (c) is to step 4), and (d) is to step 5). The data are from atmPhs_C001.2007. 055.00.18.G14_0001.0001_nc.
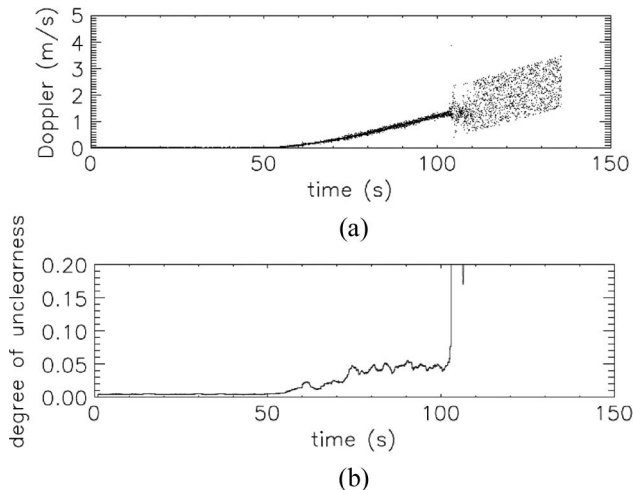

(a)

(b)

Fig. 14. (a) Doppler and (b) the degree of unclearness of the L2 RO data from atmPhs_C001.2007.055.00.18.G14_0001.0001_nc.
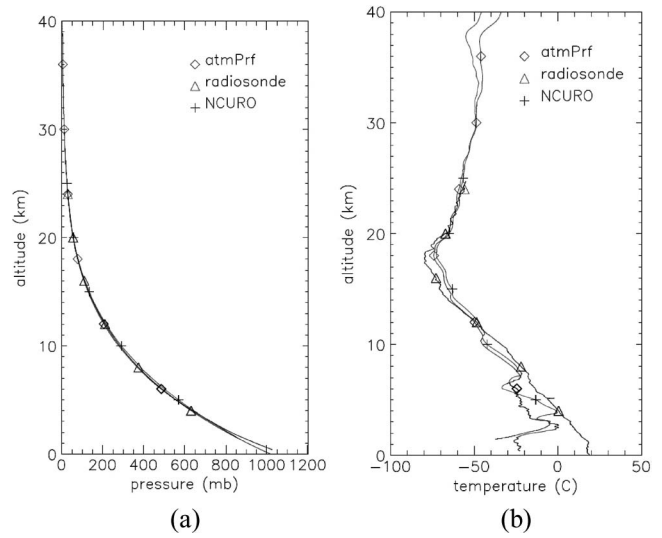

(a)

(b)

Fig. 15. Comparisons of three pressure and temperature profiles which are retrieved using the NCURO algorithm and obtained from atmPrf file and radiosonde measurement. The input of the NCURO algorithm is obtained from atmPhs_C003.2007.019.19.22.G23_2007.3200_nc, and atmPrf file is obtained from atmPrf_C003.2007.019.19.22.G23_2007.3200_nc.

files are named using the same rule for atmPhs and gpsBit files, as described in Section II. In the mentioned time period, it is able to retrieve 22 pressure and temperature profiles of the atmosphere near Taiwan. Nevertheless, considering the quality and occurrence time of the data, only limited amount of data in the atmPrf files and radiosonde measurement are available for comparison. One case with available atmPrf file and radiosonde measurement is shown in Fig. 15. Fig. 15 shows the comparisons of pressure and temperature profiles which are retrieved using the NCURO algorithm and obtained from atmPrf file and radiosonde measurement. Generally, these profiles are in good agreement, except for the portion near the Earth surface (less than 8 km in altitude). In reality, the atmosphere above the Pingtung radiosonde station, which is close to the sea, is often humid. As mentioned at the end of Section II, the outputs of the algorithm are dry pressure and dry temperature. Therefore, the discrepancy between the profiles near the Earth surface is expected.

To demonstrate the capability of the NCURO algorithm, Fig. 16 shows some intermediate results in obtaining the profiles in Fig. 15. Fig. 16(a1) and (a2) shows the L1 and L2 Doppler profiles, respectively. Since both profiles are obtained before the process of the phase correction (aforementioned in Section III), multiple lines and some randomly distributed points appear. Fig. 16(b1) and (b2) shows the L1 and L2 Doppler profiles after the phase correction. It should be noted that the navigation messages are only encoded in L1 signal (C/A code) [46], so Fig. 16(a2) and (b2) are the same. Fig. 16(c1) and (c2) shows the SNR profiles of the corresponding L1 and L2 signals, respectively. It can be seen that SNR profiles decrease with fluctuation. To obtain the better indication of data quality, the L1 and L2 profiles of data unclearness are calculated (aforementioned in Section IV) and shown in Fig. 16(d1) and (d2). The degrees of unclearness are set at 0.3 and 0.25 for L1 and L2 data, respectively. With the
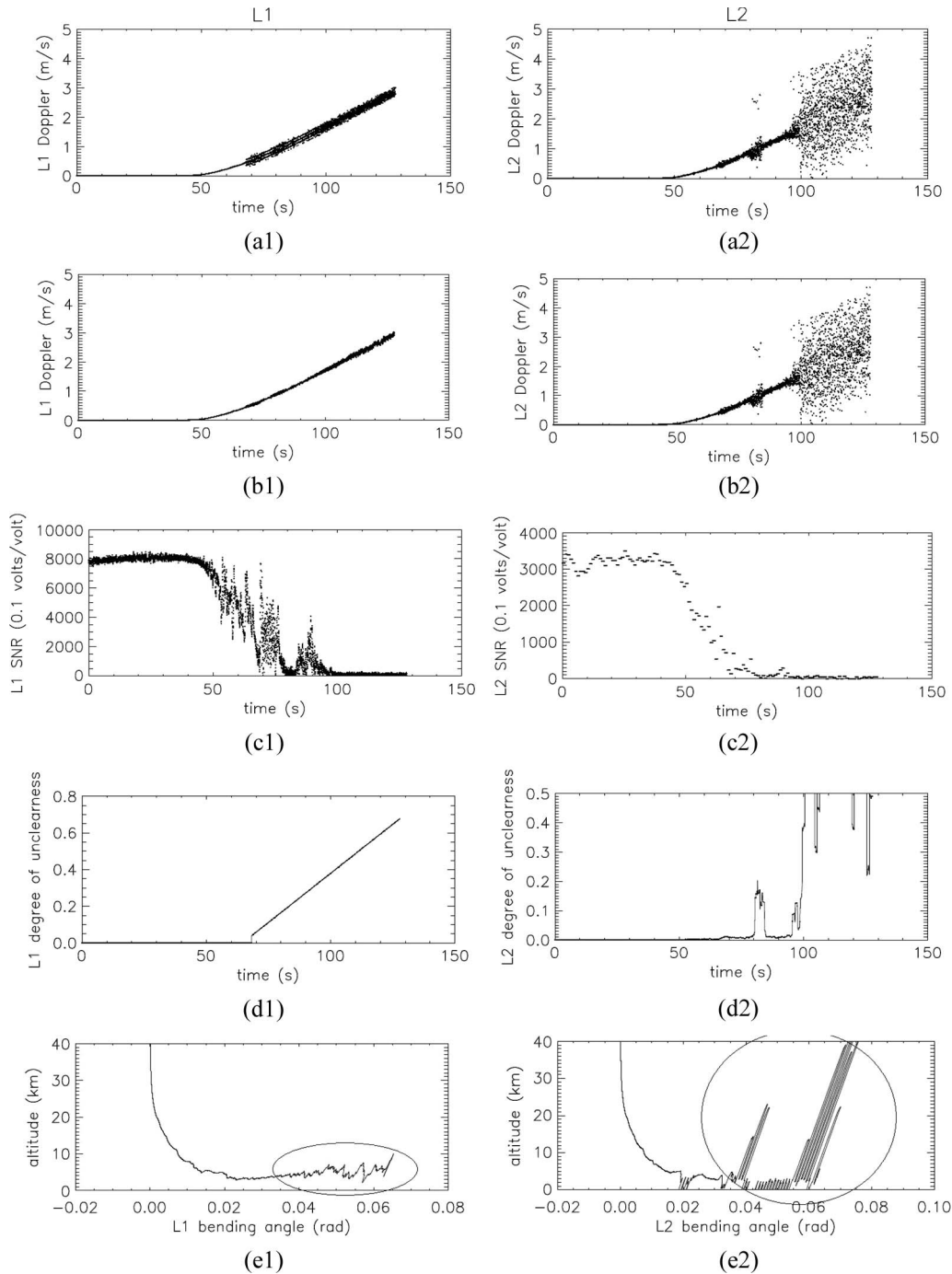
Fig. 16. Intermediate results of the profiles in Fig. 15 using the NCURO algorithm. (a1) and (a2) are L1 and L2 Doppler profiles, respectively. (b1) and (b2) are L1 and L2 Doppler after phase correction, respectively. (c1) and (c2) are SNR of L1 and L2, respectively. (d1) and (d2) are unclearness profiles of L1 and L2, respectively. (e1) and (e2) are the retrieved bending-angle profiles of L1 and L2, respectively. The circled portions are data of poor quality which have already been discarded.

criteria, the circled portions of profiles in Fig. 16(b1) and (b2) are discarded. Fig. 16(e1) and (e2) shows the retrieved L1 and L2 bending-angle profiles, respectively. The circled portions of the profiles are the data of poor quality which have already been discarded previously. With the L1 and L2 bending angles, the calibrated bending-angle profile is calculated (as aforementioned in Section II) and shown in Fig. 17. Finally, following the procedures aforementioned at the end of Section II, the pressure and temperature profiles are obtained and shown in Fig. 15.

Other comparisons between the data obtained from the NCURO algorithm and TACC are also conducted. Fig. 18 shows the profiles retrieved from the data on September 30, 2007, which is before the arrival of the typhoon Krosa. Fig. 19 shows the profiles retrieved from the data on October 5, 2007, when the typhoon Krosa hit the southeast China. Generally, the results agree well with each other. The discrepancy between the output of the NCURO algorithm and result from TACC is due to the magnitude of the noise [22]. While the magnitude of
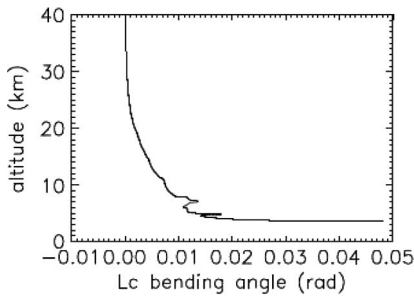
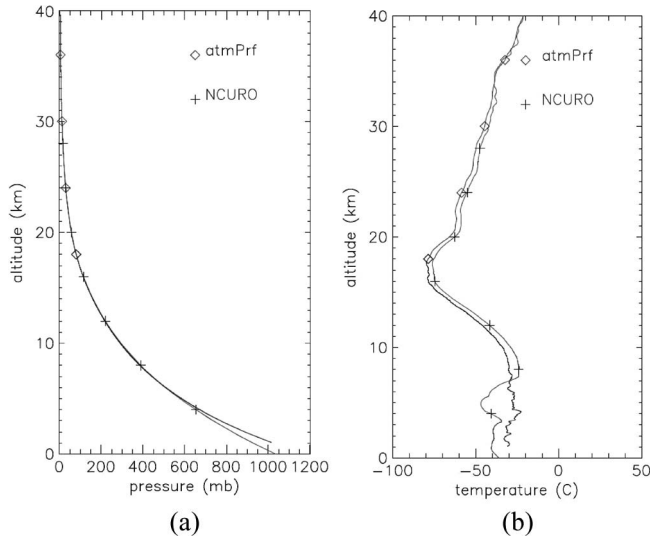Fig. 17. Calibrated bending profile from Fig. 16(e1) and (e2) using (1).

Fig. 18. Comparisons of the pressure and temperature profiles which are retrieved using NCURO algorithm and obtained from atmPrf file. The input of NCURO algorithm is obtained from atmPhs_C003.2007. 273.14.25.G23_2007.3200_nc, and atmPrf file is obtained from atmPrf_C003. 2007.273.14.25.G23_2007.3200_nc.

the bending angle and its neutral atmosphere-related variations decrease exponentially with altitude, the magnitude of the noise remains about constant and overshadows the signal above a certain altitude. To reduce the error propagation from high to low altitudes after the Abel inversion, the observational bending angle at high altitudes could be replaced by a model. So far, the NCURO algorithm described in this paper is still a theoretical algorithm, and it focuses on the improvement of the algorithm accuracy. In the future, combining the NCURO algorithm with prediction modes and weighting function of observation data will be considered in the algorithm improvement.

VI. CONCLUSION

In 2006, Taiwan launched six LEO satellites for a RO mission, FORMOSAT-3. In order to thoroughly understand the process of the data retrieval and obtain as much as possible the information for the weather prediction, a retrieval algorithm, the NCURO algorithm based on geometric optics, is developed. The focus of the algorithm development is on the correction of the signal phase received with OL technique and the criteria for the assessment of the data quality. When the OL is activated, the excess phase of the GPS signal is modulated with the navigation codes of satellites. In the algorithms, two methods
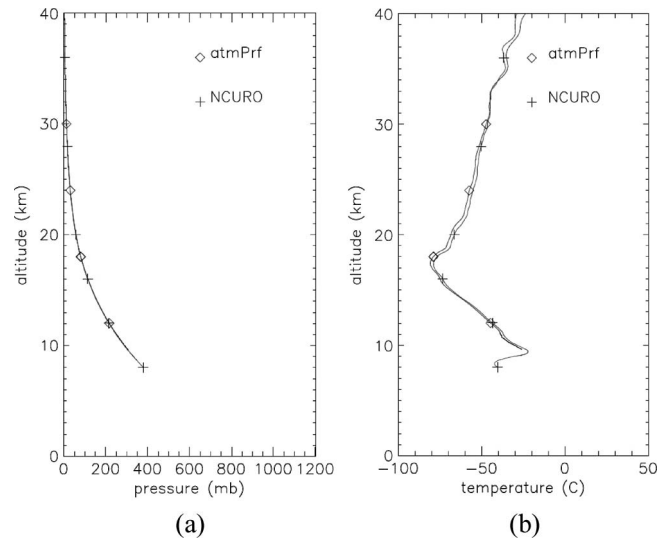

Fig. 19. Comparisons of the pressure and temperature profiles which are retrieved using NCURO algorithm and obtained from atmPrf file. The input of NCURO algorithm is obtained from atmPhs_C003.2007. 278.01.11.G03_2007.3200_nc, and atmPrf file is obtained from atmPrf_C003. 2007.278.01.11.G03_2007.3200_nc.

are incorporated to recover the excess phase. The first method can generally be used when the navigation codes of satellites can be obtained in gpsBit files. However, the navigation codes may not always be available, and then, the second method using data regression is developed to correct the excess phase in this situation. To assess the quality of the GPS signal, instead of SNR, the degree of unclearness is defined and used in the algorithm. Moreover, the degree of unclearness is the criterion to determine the quality of the signal based on the phase of the signal to reject the data of poor quality. It should be noted that the quality of the signal determines the lowest altitude at which the RO point can occur. The retrieved results from NCURO algorithm are compared with those from CDAAC at UCAR and radiosondes. Some intermediate results of the NCURO algorithm are also given in this paper to demonstrate the capability of the algorithm.

REFERENCES

[1] G. F. Lindal, J. R. Lyons, D. N. Sweetnam, V. R. Eshliman, D. P. Hinson, and G. L. Tyler, "The atmosphere of Uranus: Results of radio occultation measurements with Voyager 2," *J. Geophys. Res.*, vol. 92, pp. 14 987–15 001, Dec. 30, 1987.

[2] R. A. Phinney and D. L. Anderson, "On the radio occultation method for studying planetary atmospheres," *J. Geophys. Res.*, vol. 73, no. 5, pp. 1819–1827, 1968.

[3] Y. A. Liou, "Letter from the guest editor," *GPS Solut.*, vol. 9, no. 2, pp. 85–87, 2005.

[4] G. F. Lindal, G. E. Wood, H. B. Hotz, D. N. Sweetnam, V. R. Eshleman, and G. L. Tyler, "The atmosphere of Titan: An analysis of the Voyager 1 radio occultation measurement," *Icarus*, vol. 53, pp. 348–363, 1983.

[5] R. Ware, M. Exner, D. Feng, M. Gobunov, K. Hardy, B. Herman, Y. Kuo, T. Meehan, W. Melbourne, C. Rocken, W. Schreiner, S. Sokolovskiy, F. Solheim, X. Zou, R. Anthes, S. Businger, and K. Trenberth, "GPS sounding of the atmosphere for low Earth orbit: Preliminary results," *Bull. Amer. Meteorol. Soc.*, vol. 77, no. 1, pp. 19–40, 1996.

[6] A. G. Pavelyev, Y. A. Liou, J. Wickert, T. Schmidt, A. A. Pavelyev, and S. F. Liu, "Effects of the ionosphere and solar activity on radio occultation signals: Application to CHAllenging Minisatellite Payload satellite observations," *J. Geophys. Res.*, vol. 112, no. A6, p. A06 326, Jun. 2007.

[7] J. Wickert, C. Reigber, G. Beyerle, R. Konig, C. Marquardt, T. Schmidt, L. Grunwaldt, R. Galas, T. K. Meehan, W. G. Melbourne, and K. Hocke, "Atmosphere sounding by GPS radio occultation: First results from CHAMP," *Geophys. Res. Lett.*, vol. 28, no. 17, pp. 3263–3266, 2001.

[8] T. P. Yunck, C.-H. Liu, and R. Ware, "A history of GPS sounding," *Terr. Atmos. Ocean. Sci.*, vol. 11, no. 1, pp. 1–20, 2000.

[9] S. Synbdergaard, C. Rocken, W. S. Schreiner, and D. C. Hunt, "Ionospheric observations from the FORMOSAT-3/COSMIC GPS occultation experiment: Preliminary results," in *Proc. AGU Fall Meeting*, San Francisco, CA, 2006.

[10] Y.-A. Liou, A. G. Pavelyev, S. F. Liu, A. A. Pavelyev, N. Yen, C. Y. Huang, and C. J. Fong, "FORMOSAT-3/COSMIC GPS radio occultation mission: Preliminary results," *IEEE Trans. Geosci. Remote Sens.*, vol. 45, no. 11, pp. 3813–3826, Nov. 2007.

[11] C.-H. Lin, J. Y. Liu, T.-W. Fang, P.-Y. Chang, H.-F. Tsai, C. H. Chen, and C.-C. Hsiao, "Motions of the equatorial ionization anomaly crests imaged by FORMOSAT-3/COSMIC," *Geophys. Res. Lett.*, vol. 34, no. 19, p. L19 101, Oct. 2007.

[12] C.-J. Fong, A. Shiau, T. Lin, T.-C. Kuo, C.-H. Chu, S.-K. Yang, N. Yen, S. S. Chen, C.-Y. Huang, Y.-H. Kuo, Y.-A. Liou, and S. Chi, "Constellation deployment for the FORMOSAT-3/COSMIC mission," *IEEE Trans. Geosci. Remote Sens.—A Special Issue on 'Meteorology, Climate, Ionosphere, Geodesy, and Reflections From the Ocean Surfaces: Studies by Radio Occultation Methods'*, vol. 46, no. 11, pp. 3366–3378, Nov. 2008.

[13] C.-J. Fong, N. Yen, V. Chu, S.-S. Chen, and S. Chi, "Operations challenges from the FORMOSAT-3/COSMIC constellation for global earth weather monitoring," in *Proc. IEEE Aerosp. Conf.*, Big Sky, MT, 2007, pp. 1–14.

[14] A. G. Pavelyev, Y. A. Liou, J. Wickert, A. A. Pavelyev, T. Schmidt, K. Igarashi, and S. S. Matyugov, "Location of layered structures in the ionosphere and atmosphere by use of GPS occultation data," *Adv. Space Res.*, vol. 42, no. 1, pp. 224–228, Jul. 2008.

[15] S. Sokolovskiy, Y.-H. Kuo, C. Rocken, W. S. Schreiner, D. Hunt, and R. A. Anthes, "Monitoring the atmospheric boundary layer by GPS radio occultation signals recorded in the open-loop mode," *Geophys. Res. Lett.*, vol. 33, no. 12, p. L12 813, Jun. 2006.

[16] D. Narayana Rao, M. Venkat Ratnam, B. V. Krishna Murthy, V. V. M. Jagannadha Rao, S. K. Mehta, D. Nath, and S. Ghouse Basha, "Identification of tropopause using bending angle profile from GPS radio occultation (RO): A radio tropopause," *Geophys. Res. Lett.*, vol. 34, no. 15, p. L15 809, Aug. 2007.

[17] Y.-A. Liou and A. G. Pavelyev, "Simultaneous observations of radio wave phase and intensity variations for locating the plasma layers in the ionosphere," *Geophys. Res. Lett.*, vol. 33, L23102, 2006. DOI:10.1029/2006GL027112.

[18] Y.-A. Liou, A. G. Pavelyev, J. Wickert, T. Schmidt, and A. A. Pavelyev, "Analysis of atmospheric and ionospheric structures using the GPS/MET and CHAMP radio occultation database: A methodological review," *GPS Solutions*, vol. 9, no. 2, pp. 122–143, 2005. DOI: 10.1007/s10291-005-0141-y.

[19] C. Hwang, T. Tseng, T. Lin, C. Fu, and D. Svehla, "Precise orbit determination for FORMOSAT-3/COSMIC and gravity application," in *Proc. AGU Fall Meeting*, San Francisco, CA, 2006.

[20] Y.-A. Liou, A. G. Pavelyev, J. Wickert, S. F. Liu, and A. A. Pavelyev, "Application of GPS radio occultation method for observation of the internal waves in the atmosphere," *J. Geophys. Res.*, vol. 111, no. D6, p. D06 104, Mar. 2006.

[21] Y.-H. Kuo, S. V. Sokilovskiy, R. A. Anthes, and F. Vandenberghe, "Assimilation of GPS radio occultation data for numerical weather prediction," *Terr. Atmos. Ocean. Sci.*, vol. 11, pp. 157–186, 2000.

[22] Y.-H. Kuo, T.-K. Wee, S. Sokolovskiy, C. Rocken, W. Schreiner, D. Hunt, and R. A. Anthes, "Inversion and error estimation of GPS radio occultation data," *J. Meteorol. Soc. Jpn*, vol. 82, no. 1B, pp. 507–531, 2004.

[23] D. D. Feng and M. Herman, "Remote sensing the Earth's atmosphere using the global positioning system (GPS)—The GPS/MET data analysis," *J. Atmos. Ocean. Technol.*, vol. 16, pp. 989–1002, 1999.

[24] M. D. Mortensen and P. Hoeg, "Inversion of GPS occultation measurements using Fresnel diffraction theory," *Geophys. Res. Lett.*, vol. 25, no. 13, pp. 2441–2444, 1998.

[25] M. E. Gorbunov, "Three-dimensional satellite refractive tomography of the atmosphere: Numerical simulation," *Radio Sci.*, vol. 31, no. 1, pp. 95–104, 1996.

[26] M. E. Gorbunov and A. S. Gurvich, "Microlab-1 experiment: Multipath effects in the lower troposphere," *J. Geophys. Res.*, vol. 103, no. D12, pp. 13 819–13 826, 1998.

[27] K. Igarashi, A. Pavelyev, J. Wickert, K. Hocke, and D. Pavelyev, "Application of radio holographic method for observation of altitude variations of the electron density in the mesosphere/lower thermosphere using GPS/MET radio occultation data," *J. Atmos. Sol.-Terr. Phys.*, vol. 64, no. 8–11, pp. 959–969, May 2002.

[28] A. G. Pavelyev, Y.-A. Liou, C. Reigber, J. Wickert, K. Igrashi, K. Hocke, and C. Y. Huang, "GPS radio holography as a tool for remote sensing of the atmosphere and mesosphere from space," *GPS Solut.*, vol. 6, no. 1/2, pp. 100–108, 2002.

[29] A. G. Pavelyev, T. Tsuda, K. Igarashi, Y.-A. Liou, and K. Hocke, "Wave structures in the electron density profile in the ionospheric D- and E-layers observed by radio holography analysis of the GPS/MET radio occultation data," *J. Atmos. Sol.-Terr. Phys.*, vol. 65, no. 1, pp. 59–70, Jan. 2003.

[30] A. S. Jensen, M. S. Lohmann, H.-H. Benzon, and A. S. Nielsen, "Full spectrum inversion of radio occultation signals," *Radio Sci.*, vol. 38, no. 3, p. 1040, 2003.

[31] M. E. Gorbunov, "Ionospheric correct and statistical optimization of radio occultation data," *Radio Sci.*, vol. 37, no. 5, p. 1084, 2002.

[32] Y.-A. Liou and C.-Y. Huang, "Active limb sounding of atmospheric refractivity and dry temperature profiles by GPS/Met occultation," in *Proc. COSPAR Colloquia Series*, Taipei, Taiwan, 2002, vol. 12, pp. 325–328.

[33] C. Y. Huang, "Data retrieval of GPS radio occultation," Ph.D. dissertation, Inst. Space Sci., Nat. Central Univ., Taiwan, 2005. (Thesis advisor: Dr. Yuei-An Liou).

[34] S. V. Sokolovskiy, "Tracking tropospheric radio occultation signals from low Earth orbit," *Radio Sci.*, vol. 36, no. 3, pp. 483–498, 2001.

[35] [Online]. Available: http://tacc.cwb.gov.tw/cdaac/fileFormats/gpsBit.html

[36] [Online]. Available: http://cosmic-io.cosmic.ucar.edu/cdaac/fileFormats/index.html

[37] S. Syndergaard, "Modeling the impact of the Earth's oblateness on the retrieval of temperature and pressure profiles from limb sounding," *J. Atmos. Sol.-Terr. Phys.*, vol. 60, no. 2, pp. 171–180, Jan. 1998.

[38] R. E. Ziemer and W. H. Tranter, *Principles of Communications: Systems, Modulation, and Noise*, 5th ed. Boston, MA: Houghton Mifflin, 2001.

[39] A. Leick, *GPS Satellite Surveying*, 3rd ed. Hoboken, NJ: Wiley, 2004.

[40] G. Fjeldbo and A. J. Kliore, "The neutral atmosphere of Venus as studied with the Mariner V radio occultation experiments," *Astron. J.*, vol. 76, no. 2, pp. 123–140, 1971.

[41] V. V. Vorob'ev and T. G. Krasil'nikova, "Estimation of the accuracy of the atmospheric refractive index recovery from Doppler shift measurements at frequencies used in the NAVSTAR system," *Phys. Atmos. Ocean*, vol. 29, no. 5, pp. 602–609, 1994.

[42] R. A. Phinney and D. L. Anderson, "On the radio occultation method for studying planetary atmospheres," *J. Geophys. Res.*, vol. 73, no. 5, pp. 1819–1827, 1968.

[43] G. D. Thayer, "An improved equation for the radio refractive index of air," *Radio Sci.*, vol. 9, no. 10, pp. 803–807, 1974.

[44] [Online]. Available: http://tacc.cwb.gov.tw/cdaac/login/cosmic/

[45] S. Sokolovskiy, "Open loop tracking and inverting GPS L1 radio occultation signals: Simulation study," in *Occultations for Probing Atmosphere and Climate*, G. Kirchengast, U. Foelsche, and A. K. Steiner, Eds. New York: Springer-Verlag, 2004, pp. 39–51.

[46] B. Hofmann-Wellenhof, H. Lichtenegger, and J. Collins, *Global Positioning System, Theory and Practice*, 5th revised ed. New York: Springer-Verlag Wien, 2001.

Tsen-Chieh Chiu (M'98) received the B.S. and M.S. degrees from the National Taiwan University, Taipei, Taiwan, in 1990 and 1992, respectively, and the Ph.D. degree from the University of Michigan, Ann Arbor, in 1998.

He is currently an Associate Professor with the faculty of the Department of Electrical Engineering, National Central University, Taoyuan, Taiwan. His research interests include microwave remote sensing, electromagnetic scattering problems, and the design and analysis of microwave circuits.

Yuei-An Liou (S'91–M'96–SM'01) received the B.S. degree in electrical engineering from the National Sun Yat-Sen University, Kaohsiung, Taiwan, in 1987 and the M.S.E. degree in electrical engineering, the M.S. degree in atmospheric and space sciences, and the Ph.D. degree in electrical engineering and atmospheric, oceanic, and space sciences from the University of Michigan, Ann Arbor, in 1992, 1994, and 1996, respectively.

From 1989 to 1990, he was a Research Assistant with the Robotics Laboratory, National Taiwan University, Taipei, Taiwan. From 1991 to 1996, he was a Graduate Student Research Assistant with the Radiation Laboratory, University of Michigan, where he developed land–air interaction and microwave-emission models for prairie grassland. He was with the faculty of the Center for Space and Remote Sensing Research (CSRSR) in 1996, with the Institute of Space Sciences in 1997, and with the Department of Electrical Engineering in 2005 at the National Central University (NCU), Taoyuan, Taiwan, where he is currently a Professor and also the Director of CSRSR. He served as the Division Director with the Science Research Division, National Space Organization (NSPO) of Taiwan in 2005 and continued to serve as Advisor in 2006. From August 2006 to July 2007, he was a Chair Professor and the Dean of the College of Electrical Engineering and Computer Science, Ching Yun University, Jhongli, Taiwan. His current research activities include GPS meteorology and ionosphere, remote sensing of the atmosphere and land surface, land-surface processes modeling, and application of neural networks and fuzzy systems in inversion problems. He is a Principal Investigator on many research projects sponsored by the National Science Council (NSC), Council of Agriculture, and NSPO, Civil Aeronautics Administration, Minister of Interior, Water Conservancy Agency of Taiwan, and Office of Naval Research of U.S. He has over 70 referral papers and more than 200 international conference papers.

Dr. Liou is a Referee for *Terrestrial, Atmospheric and Oceanic Sciences*, IEEE TRANSACTIONS ON GEOSCIENCE AND REMOTE SENSING (TGRS), *Asian Journal of Geoinformatics, International Journal of Remote Sensing, Earth, Planets, and Space, Water Resources Research, Environmental Modelling and Software, Remote Sensing of Environment, J. Geophys. Res., and Annales Geophysicae.* He is a member of the Editorial Advisory Board to *GPS Solutions* and serves as Guest Editor for the June 2005 Special Issue of "GPS Radio Occultation (RO) Experiments" of GPS Solutions. In addition, he serves as a leading Guest Editor for the IEEE TGRS Special Issue "Meteorology, Climate, Ionosphere, Geodesy, and Reflections from the Ocean surfaces: Studies by Radio Occultation Methods." He also serves as Associated Editor, IEEE-JSTARS starting from 2008. He is listed in Who's Who in the World. He was the recipient of Annual Research Awards from NSC in 1998, 1999, and 2000, the recipient of The First Class Research Awards from NSC in 2004, 2005, and 2006, and the recipient of NCU Outstanding Research Awards in 2004 and 2006. He was the recipient of the "Contribution Award to FORMOSAT3 National Space Mission" from NSPO in 2006. He is a member of the American Geophysical Union, the American Meteorological Society, and the International Association of Hydrological Sciences. He was the recipient of the Honorary Life Member of The Korean Society of Remote Sensing in 2007. He was elected as Foreign Member, Russian Academy of Engineering Sciences, in 2008. He was the recipient of the Outstanding Alumni Award from the University of Michigan Alumni Association in Taiwan in 2008.

Wen-Hao Yeh was born in Taiwan, in 1979. He received the B.S. degree in physics and the M.S. degree in astronomy from the National Central University, Taoyuan, Taiwan, in 2002 and 2005, respectively. He is currently working toward the Ph.D. degree in electrical engineering at the National Central University, Taoyuan, Taiwan.

His research interests include numerical simulation and analysis, retrieval technology, and gravity wave activity.

Cheng-Yung Huang received the B.S., M.S., and Ph.D. degrees from the Institute of Space Science, National Central University, Taoyuan, Taiwan, in 1995, 1997, and 2005, respectively.

He is currently with the Institute for Scientific Research, Boston College, Chestnut Hill, MA. His research interests include radio occultation, global positioning system, and satellite remote sensing.